

# **Ground Truthing Earth's Silicate Weathering Thermostat: Using the Geochemistry of Himalayan Groundwaters to Calculate Residence Times**

Giovanni Bernardi

Part III Project

2024-2025



# **Abstract**

IMO, the abstract should be a supercondensed version of the paper.

Grab the readers attention -> why we care about the topic

What's the unknown? Are fluids actually following the Maher model?

How did you do this? Collected samples, tested models.

What did you find? The Maher model isn't appropriate etc

Loop back into the original part about why we care and the unknown. Has it been answered? What are the implications?

Residence time calculations determined using rate constants close to equilibrium give ages of order ten years for the model which purports discharge to be the greatest control on weathering. The other model, following the null hypothesis that temperature is the greatest control on weathering, gives residence times of a similar order of magnitude but the assumption of a constant rate of reaction is likely unrealistic. Simple calculations based on yearly rainfall support the residence time obtained by both models. Estimates of free energy suggest that the weathering reactions contributing to the dissolved load in the groundwater are not close to equilibrium. As a result, it is unlikely that the fast rates of reaction used are appropriate for catchments like Melamchi. Furthermore, this suggests that the main assumption of the Maher model is not valid in this catchment. These analyses suggest that a combination of both models' is necessary to accurately model a real catchment like Melamchi.

# **Contents**

## **Acknowledgements**

This thesis would not have been possible without the amazing help from my supervisor, Ed Tipper. Mike Bickle and Al Knight and Morag Hunter have also been instrumental in guiding me through this Master's year. To Zara, I couldn't ask for a better field partner. To my friends and peers, thank you for supporting me throughout. A Mamma, Papà, e la Virgi, grazie di tutto come sempre. And finally, Beth,

## **List of Tables**

# **Nomenclature**

# 1 Introduction

Silicate weathering, whereby silicate minerals are dissolved by carbonic acid, sequesters atmospheric CO<sub>2</sub> over long (10<sup>6</sup> year) timescales, influencing global climate regulation. As water passes through the subsurface, it interacts with the surrounding rock. This causes the addition of solute species to the groundwater, and the formation of stable secondary minerals through the dissolution of primary minerals. Large mountain ranges in particular are thought to be most sensitive to weathering (Tipper et al., 2006). The Himalayan mountain range spans more than 590,000 km<sup>2</sup>, and is the source of major rivers, including the Ganges, Brahmaputra, and Indus. The dissolution kinetics of the silicate rocks in Himalayan catchments are thought to be sensitive to temperature and runoff because the weathering reactions have not gone to completion. Silicate weathering in the Himalayas as a result of their uplift and erosion in the Cenozoic may have contributed significantly to the global cooling over the past 40 million years (Raymo and Ruddiman, 1992; West et al, 2005, Kump et al, 2000). Clearly, understanding the strongest control on weathering in these key regions for the global carbon cycle is of utmost importance to inform climate policy. In highly erosive regions like the Himalayas where the supply of silicate minerals far exceeds the weathering rate, silicate weathering reactions are thought to be more sensitive to temperature than runoff. These are regions are called "kinetically-limited" (Stallard & Edmund 1983 JGR, West et al, 2005). Reactive transport models are widely used in Earth Sciences to simulate the flow of groundwater through the subsurface (Bethke, 2011). Reactive transport models built on this temperature sensitivity ("Fontorbe models" from now on, after Fontorbe et al., 2013) are used to simulate groundwater through one-dimensional flow paths based on a few key parameters, which make up the "weathering fingerprint" of a catchment. More recent models have proposed silicate weathering is more sensitive to runoff than to temperature (Maher, 2011). These ("Maher models" from now on, after Maher, 2011) assume that all weathering paths approach equilibrium. This study looks at Melamchi, a Himalayan catchment north-east of Kathmandu in Nepal, to act as a case study for Himalayan weathering. Determining the greatest control on weathering in Melamchi is complicated, however, and a proxy is needed for the comparison of the two models.

Estimation of residence time from the Maher and Fontorbe models using measured spring chemistry in Melamchi will act as the proxy for weathering control. The weathering fingerprints of these catchments contain many unknowns, namely the residence time of the water, flow path direction and length, rate of reaction, and extent to which equilibrium is reached. Spring chemistry is reflective of the weathering processes that occur in the subsurface, and can therefore be used to estimate these fingerprint parameters. Residence time, also called the advective age, is defined by how long a given water packet spends from rain recharge into groundwater to exiting at a spring (McCallum et al, 2015). Understanding residence time in particular is important because the geochemical and biogeochemical reactions that contribute to the solute load during weathering are time-dependent; generally, longer residence times promote greater solute accumulation in the water (Berner, 1978). These geochemical reactions are also controlled by the reaction rate which is thought to vary as equilibrium is approached (White and Brantley, 2003; Maher, 2011). Therefore, an understanding of residence time will provide insight into how long weathering reactions take place in a given catchment, whether they reach equilibrium, and what this means for the carbon cycle as a whole. Residence time will also reflect the variety of flow routes within a catchment because of physical constraints like Darcy's law, which will help to improve hydrological models. Calculating residence time using the spring chemistry in Melamchi will allow the assumptions underlying the two models to be tested, and assess their applicability to a real-world catchment.

From the model comparison will also come a better understanding of fluid residence times in Himalayan catchments, for which tracer data is already commonly used to infer how long a water packet spends in the subsurface (Atwood et al, 2021). Previous studies on Melamchi have used CFC and SF<sub>6</sub> gases to determine a mean age on the order of ten years for groundwater at the base of the catchment ridge (Atwood et al, 2021) (ref map). Using the chemical composition of the water will provide a different way of obtaining residence times, and give a benchmark for the tracer data, which is often reported to be limited in its application (McCallum et al, 2015). If the residence time of a particular water packet is long enough, the reaction will reach chemical equilibrium, meaning the free energy of the sys-

tem will be close to zero (Kampman et al., 2013). Comparison of these residence times with separate estimates of free energy derived from the measured concentration of springwater in the catchment will test the validity of the two models and their assumptions. Finally, this will help to inform whether weathering in catchments like Melamchi is most strongly controlled by temperature or runoff.

The rate of weathering is dependent on the mineralogy of the rock. Different minerals weather at different rates. Therefore, the most reactive minerals will disproportionately contribute to the solute load of the water (Shand et al, 1999). Differences in lithology are therefore also thought to affect weathering. Geological differences lead to differences in soil composition, landscape features, vegetation, and climate which in turn affect the rates of reaction. Logically, the contribution of one lithology to weathering is at least in part correlated to its spatial extent in the catchment (Stallard and Edmond, 1983). In the Melamchi catchment, only weathering through carbonic acid is considered. Weathering through sulfuric acid also significantly contributes to the global weathering budget, but its impact is not considered in this study because the marine deposits required for its formation are not present in the Melamchi region (Bufo et al., 2021).

Weathering regimes can be classified as either transport-limited or kinetically limited (West et al., 2005). West et al. (2005) distinguish the two regimes by the rate of erosion in the catchment. In low erosion rate settings, weathering is transport-limited due to limited mineral supply. Weathering here is proportional to the material eroded. In high erosion rate settings, weathering is kinetically-limited due to an abundant mineral supply. Rapidly eroding catchments like Melamchi are likely kinetically-limited. Soil properties and topography can be used to identify different weathering regimes in the subsurface (Pedrazas et al, 2021). Indeed, bedrock strength is thought to be more dependent on weathering than mineral or textural differences between the metamorphic lithologies in the Himalayas (Medwedeff et al, 2021). Understanding the extent of weathering can therefore also serve to predict the stability of bedrock in rapidly eroding regions.

Estimation of porosity is essential for understanding the extent of weathering in a catchment. Understanding how open a rock is to water flow and reaction can constrain the reactive transport models used to estimate residence time. Porosities vary widely across a catchment depending on the rock type encountered (Singh et al, 1987; David et al, 1994). Porosity also increases as a rock becomes more weathered (Marques et al, 2009). Note that in the following models, the porosity value is taken to be an average over a given depth in the subsurface. In Earth Sciences, models of fluid flow – whether in the subsurface or deep within the Earth – are typically categorized based on whether the flow occurs through a porous medium or within large open channels (Pedrazas et al, 2021; Maher, 2011; Kelemen et al, 1999; Jackson et al., 2018). This remains an open debate beyond the scope of this study (though note that in later sections flow paths are depicted as "channels" to facilitate the explanation of reactive transport). Hence, the porosity value used for residence time calculation is assumed to be an average. This allows for both types of flow to be plausible, whether in a highly porous medium or large channels surrounded by less porous rock.

Rates of reaction during weathering comprise both dissolution and precipitation, and chemical equilibrium is defined as that state where these are balanced and equal. Rates of reaction are thought to be different depending on whether they are measured in the field or in a laboratory (Maher et al., 2009). This difference has been explained by denoting 'extrinsic' qualities that are variable in the field, such as permeability, mineral/fluid ratios and different surface areas available to react (White and Brantley, 2003). The rate of reaction of a system has also been linked to the free energy of the system, with laboratory rates being calculated significantly further away from equilibrium than field rates (Kampman et al, 2009). This implies that field localities are closer to equilibrium than laboratory-derived rates might suggest.

The strontium isotope composition of different rock types is indicative of different formation mechanisms and conditions. This is used to track the relative contributions of weathering and hydrothermal circulation inputs in seawater (Edmond, 1992). The rock signature imparts a strontium isotopic composition to groundwater that reacts with it in the subsur-

face. Hence, measuring the strontium isotopic composition of springs can provide information on provenance and mixing between groundwaters that react with different lithologies (Faure, 2001).

The Indian Summer Monsoon (ISM) in Nepal is characterised by a strong seasonal reversal of winds, which brings heavy rainfall to the region during the summer months, and dry conditions during the winter (Bookhagen and Burbank, 2010). The monsoon brings a large amount of precipitation to the region. Oxygen isotope measurements suggest most of the precipitation occurs in the higher elevation parts of the catchment, and this is supported by remotely sensed rainfall estimates in the region (Acharya et al, 2020; Bookhagen and Burbank, 2010). Precipitation and discharge relationships in the Himalayas have been used to suggest that there is a three month lag in the response of the river to precipitation (Andermann et al., 2012). The residence time of groundwater can be used to quantify this delay and nature of its origin, given that rain is the main source of recharge to the groundwater system (Illien et al, 2021). Seasonal variation in rainfall is thought to relate to different hydrological regimes, whereby river discharge and precipitation are 'coupled' when there is a significant enough amount of water to recharge the groundwater system. (Illien et al, 2021) The seasonal variation in precipitation therefore also translates to a variation in runoff, whereby this is twelve times stronger during the monsoon than during the dry season (Sharma, 1997).

Changes in climate contribute to changes in the monsoonal system dynamics. The start of the monsoon has not changed in Nepal, but the end has been delayed. This has led to more intense precipitation on a per day basis, which is detrimental for crops in the winter season due to lack of moisture. Intense precipitation is also considered the main climatic cause of flooding (Panahi et al, 2015; Baniya et al, 2012). "One-off" landslide events transport as much as four times the flux of sediment deposited in the valley in a year (Chen C et al., 2023). These events are thought to be increasing in frequency over recent years as a result of climate change, increasing the erosion rate in these areas (Adhikari et al, 2023). In particular, effects of a flash flood in 2021 are still visible in the area, with damage done

to several bridges and hundreds of families.

In this study, spring and rain samples from the Melamchi region of Nepal are used as a case study to investigate the weathering rates in a kinetically-limited catchment. (ref map) The sample dataset consists of 372 samples spanning four field campaigns over three years (2021-2024), as well as more recent year-long bi-weekly timeseries data from stream and spring samples in sites across the catchment. Of those, 68 were collected in September 2024 by a team with researchers from the University of Cambridge and Kathmandu University for this study. This dataset comprises major ion concentrations, alkalinity, and radiogenic strontium isotopes from the Melamchi catchment.

## **2 Study Area**

The Melamchi-Indrawati catchment (85.441 - 85.601 E, 27.822 - 28.157 N) study area ranges from 790 to 5700 m a.s.l. (metres above sea level). The Melamchi River is a tributary of the larger Indrawati River and runs through the catchment draining an area of 325km<sup>2</sup>.

### **2.1 Geology and Geomorphic Setting**

The geology of Melamchi is characterised by the characteristic banded gneiss, feldspathic schist and laminated quartzite of the Higher Himalayan Crystalline Sequence (HHCS). To the south of the confluence of the Melamchi River to its parent Indrawati river lies the Main Central Thrust (MCT) which separates the HHCS from the Lower Himalayan Sequence (LHS) (Dhital et al, Graf et al). The overall geology is therefore largely comprised of silicate metamorphic rock. (map)

### **2.2 Climate**

Annual mean temperatures in the Melamchi Khola Catchment range from 24°C at base elevation to 8°C at highest elevation sampled (3200 m a.s.l.). The area is characterised by a high erosion rate. The southern Himalayas are characterised by a large topographic gradient. This corresponds to a large temperature gradient contributing to tropical and alpine climates close to one another (Kattel et al, 2012). The westerly winds typical of this latitude are responsible for the dry season in the Himalayas (Bookhagen and Burbank, 2010). The source of precipitation during the Indian Summer Monsoon (ISM) affecting Melamchi is the Bay of Bengal, due to the strong pressure gradient that changes the westerly winds to southerly winds. This temperature gradient reverses in the winter, when the oceans are warm and the High Himalaya is cold. The Melamchi Khola catchment receives over 80% of its rainfall during the monsoon.

Recorded temperatures at the end of the spring flow paths vary with the season, being coldest in November. All seasons show a temperature decrease with increasing elevation,

consistent with the free-air moist adiabatic lapse rate, which is = 6.5 °C/km (Barry and Chorley, 2009). This differs from the annual mean lapse rate in the southern Himalayas of = 5.2 °C/km (Kattel et al., 2013). This disparity could be due to the fact that temperatures may be warmer than air temperatures because of radiative heating. The difference may also be due to systematic errors in temperature measurements; between collection and sampling, warming of the water is plausible.

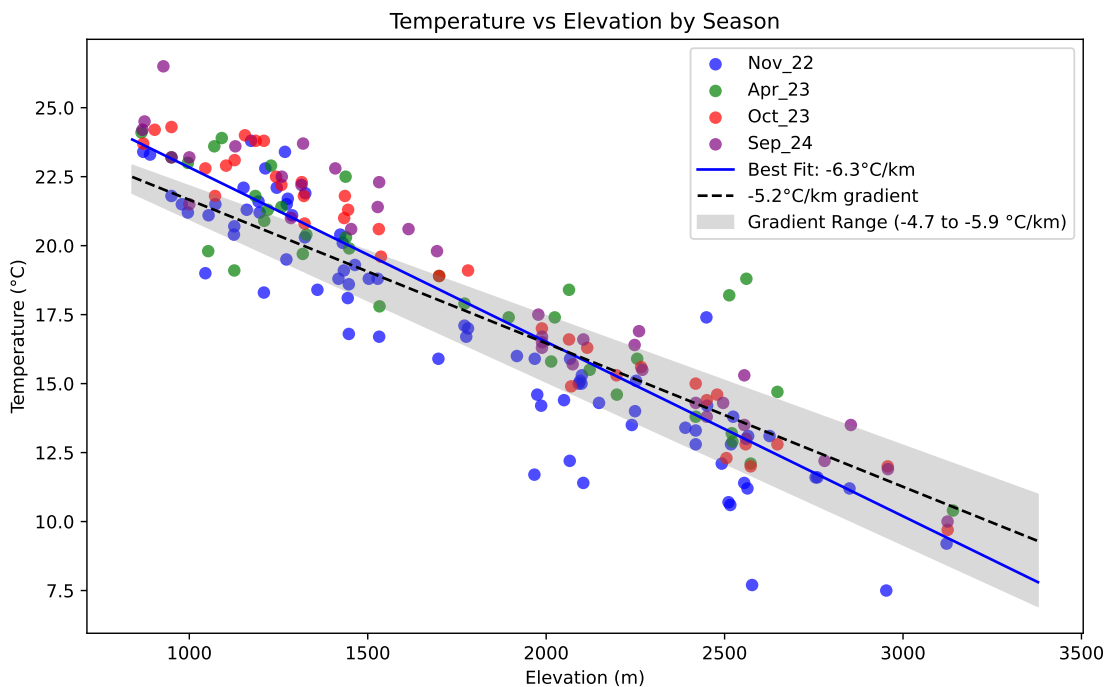


Figure 1: Temperature changes

Catchment	Area	Mean	Mean Ele-	Elevation	Geology	Location	Range
		Slope	vation	Range	(DD)		
	(km <sup>2</sup> )	(%)	(m)	(m)			
Melamchi Khola	325	20	2400	786–5697	HHCS	85.441–85.601 E 27.822–28.157 N	

Table 1: Catchment characteristics of the study area.

### **3 Data Collection and Measurement**

#### **3.1 Field Sampling**

Both springs and rain were sampled in the field. Springs were sampled according to locations visited in past expeditions. Rain was collected in a rain gauge along several transects. Both water bodies were measured in the field for temperature, pH and TDS on a Hanna Instruments HI-991300 and EXTECH DO700. Samples were also titrated using a Hach digital titrator with 0.0625M HCl to calculate the alkalinity of the water following the Gran Method (Gran, 1952). The field measurements were done 24 hours within having been collected. Six aliquots were collected for each spring for anion, cation, titration, DIC, isotope and archive purposes respectively. Rain samples had a smaller yield and so only three aliquots were collected, for ion, isotope and archive purposes. Both water body types were filtered through a  $0.2\mu\text{m}$  PES membrane in a filtration unit prior to bottling. Cation and archive samples were acidified with concentrated  $\text{HNO}_3$  to give a pH of  $\sim 2$ , keeping the cations in solution.

#### **3.2 Major and Trace Element Analysis**

Cation concentrations were determined using a Agilent Technologies 5100 Inductively-Coupled Plasma Optical Emission Spectrometer (ICP-OES) using a calibration line made from a Nepalese spring stock solution. Anion concentrations were determined using a Dionex Ion Chromatography System (ICS) 5000 series against the Battle-02 standard calibration line. Associated uncertainties range between 5-10% for cations and anions.

#### **3.3 Isotope Analysis**

Samples for radiogenic strontium analysis were dried down to provide at least 100 ng of Sr. Samples were then dissolved in aqua regia (3:1  $\text{HNO}_3:\text{HCl}$ ) to remove any additional organic matter. Once dried down again, they were added to 3 ml teflon columns with Eichrom SrSpec<sup>®</sup> resin pipetted in. Once washed three times with Milli-Q<sup>®</sup> water, the column was

primed with 3M HNO<sub>3</sub>. The sample was centrifuged then loaded onto the column avoiding any solids. The column was then washed a total of three times with 3M HNO<sub>3</sub> to remove other cations. Lastly, the column was eluted to a beaker with Milli-Q® water to collect the Sr. Once dried, the samples were dissolved in 3M HNO<sub>3</sub>, centrifuged and then diluted for analysis on a Thermo Scientific Neptune Plus MC-ICP-MS. Errors on Sr isotope measurement are taken from two standard deviations of the measured values given by the MC-ICP-MS.

## 4 Methods and Models for Analysis

### 4.1 Rain and Hydrothermal Correction

Rain input is a significant factor in the chemical composition of groundwater and rivers. Most chloride found in these water bodies is thought to be due to rainwater input (Drever, 1997). It is standard practice to correct for this rain input. Once the samples have been corrected for rain input, the remaining chloride is assumed to be derived from hydrothermal signatures encountered in the flow path. Spring waters are also therefore corrected for hydrothermal input, so that the concentrations used for modelling are strictly derived from weathering reactions.

### 4.2 Modal Decomposition Identifies Weathering Reaction

The first step towards quantifying the extent to which chemical weathering reactions have gone to completion is to discern what reaction is taking place. In principle this is as simple as knowing what minerals are dissolving and which are precipitating. Modal decomposition methods consider several minerals that could be dissolving and/or precipitating, and their stoichiometry (Garrels and Mackenzie, 1967; Drever, 1997). Note that this calculation can only be done if the number of components is the same as or greater than the number of minerals.

$$\begin{array}{ccccccc}
& Biot & Plag & Calc & Smec & Kaol & Kspar \\
\begin{matrix} Si \\ Al \\ Mg \\ Ca \\ Na \\ K \end{matrix} & \left( \begin{array}{cccccc} a_{11} & a_{12} & a_{13} & a_{14} & a_{15} & a_{16} \\ a_{21} & a_{22} & a_{23} & a_{24} & a_{25} & a_{26} \\ a_{31} & a_{32} & a_{33} & a_{34} & a_{35} & a_{36} \\ a_{41} & a_{42} & a_{43} & a_{44} & a_{45} & a_{46} \\ a_{51} & a_{52} & a_{53} & a_{54} & a_{55} & a_{56} \\ a_{61} & a_{62} & a_{63} & a_{64} & a_{65} & a_{66} \end{array} \right) & \cdot & \left( \begin{array}{c} x_{Biot} \\ x_{Plag} \\ x_{Calc} \\ x_{Smec} \\ x_{Kaol} \\ x_{Kspar} \end{array} \right) & = & \left( \begin{array}{c} b_1 \\ b_2 \\ b_3 \\ b_4 \\ b_5 \\ b_6 \end{array} \right)
\end{array}$$

Matrix algebra facilitates the calculations of the mineral proportions in the water. Given known matrices  $A$  and  $B$ , where  $A$  represents the stoichiometric quantities of elements in a mineral, and  $B$  the concentrations of elements in the water:

$$AX = B \quad (1)$$

$$X = A^{-1}B \quad (2)$$

The matrix  $X$ , corresponding to volumetric proportions of the minerals in the water, can then be calculated, under the assumptions that all minerals dissolve in a congruent fashion. Modal decomposition for spring waters was performed according to stoichiometric proportions from Bickle et al. (2015). For ease of visualisation, Figure ?? shows the positive, dissolved minerals on the LHS, and the negative, precipitated minerals on the RHS.

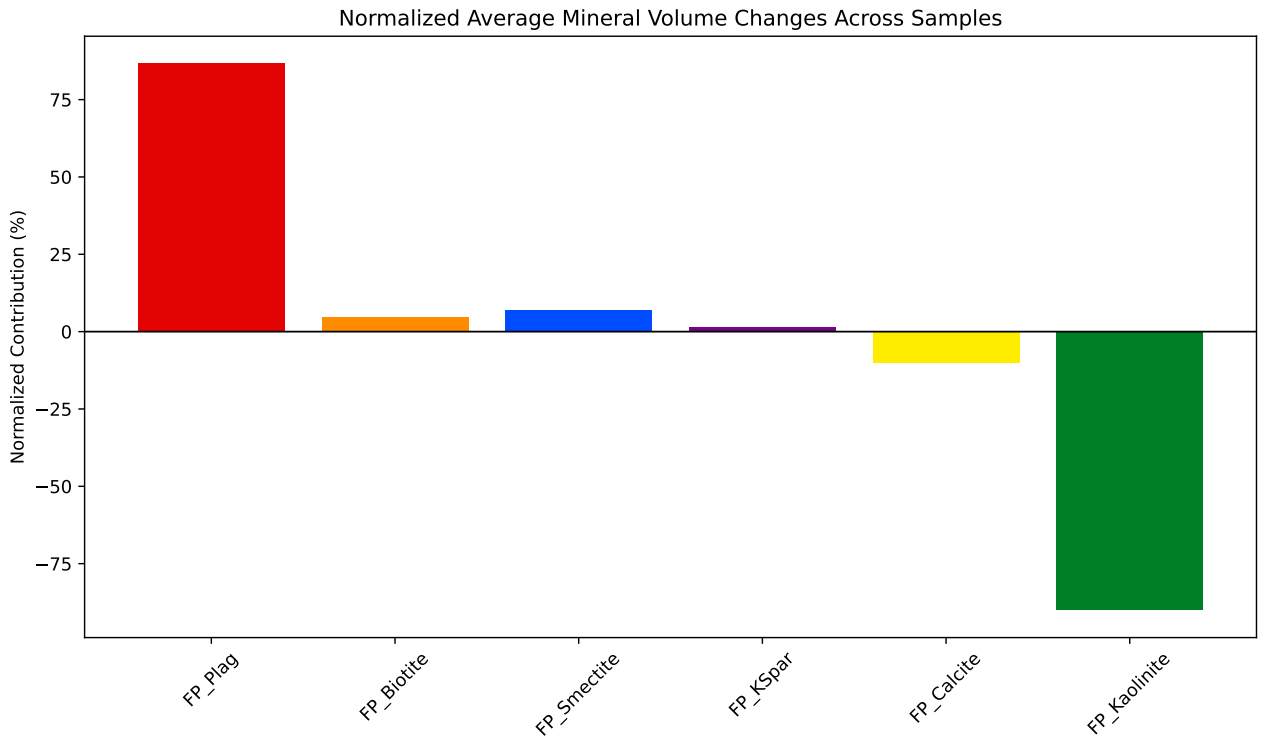
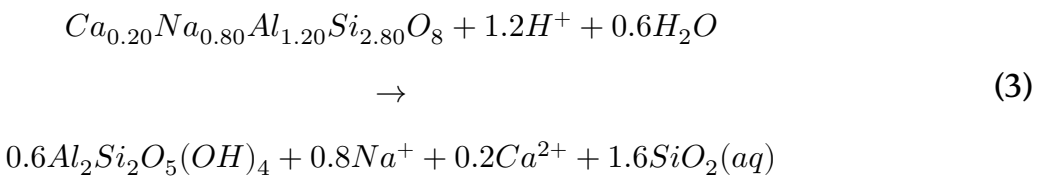
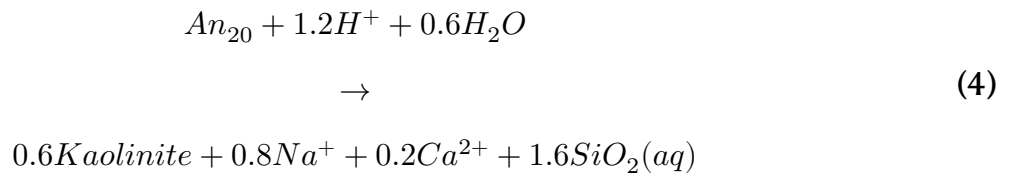


**Figure 2:** Average of the modal decomposition for the springs in Traverse 3.

Figure ?? is representative of most springs in Traverse 3. Hence, the major phase being dissolved is plagioclase feldspar and the major phase being precipitated is kaolinite. The primary composition of plagioclase in the area corresponds to  $\approx$  An-20 (Bickle et al., 2015; Knight et al., 2024). The plagioclase to kaolinite reaction is given by the following equation (written so that aluminium is conserved):



Or



## 4.3 One-Dimensional Reactive Transport Models

Reactive transport models are widely used in applied fluid dynamics and various fields within Earth Sciences. These models aim to track chemical reactions occurring at each spatial point, accounting for the movement of reactants to and reaction products away from those points (Bethke, 2011). The basic form of a reactive transport model is a partial differential equation that describes the transport of solutes and the reactions that occur between them. For reacting solutes, concentration changes over time are governed by transport rates – derived from the divergence principle – and the relative rates of dissolution and precipitation (Bethke, 2011). The proposed equations can be complex, but in simple cases a species of concentration  $C_i$  can be modelled to follow a first-order rate law, generally represented by:

$$\frac{\partial C_i}{\partial t} = \mathcal{O}_T(C_i) + \mathcal{O}_R(C_i) \quad (5)$$

Where  $\mathcal{O}_T$  and  $\mathcal{O}_R$  are the transport and reaction operators, respectively (Bethke, 2011). Depending on the hypothesis supported, equation ?? can be modified accordingly. The following sections will discuss two models with their own versions of equation ??.

### Model Motivation

As discussed in the Introduction (ref), there are different hypotheses regarding the major controls on chemical weathering. This section will contrast one model following the null hypothesis that weathering is largely sensitive to climate and temperature (Fontorbe et al., 2013), and another model that suggests weathering is more sensitive to fluid flux (Maher, 2011; Maher and Chamberlain, 2013). Given the emphasis on deriving fluid residence times from solute concentrations, the benchmark for a model's effectiveness will be how well it can predict these times compared to previous studies on gas tracers and simple box models. Assumptions and constraints will be compared and contrasted, and their results used to inform the calculation of rates of reaction and approach to equilibrium in Melam-

chi. For both models, the element used to benchmark is dissolved silicon. This is because silicon is present in both dissolution and precipitation reactions, so it is applicable to the Maher model which considers both reactions. Furthermore, silicon is what both models were used for in their respective original studies.

### **Fontorbe et al. (2013) - Model**

This model investigates silicon isotopic composition in the Ganges River, assuming constant reaction rates along flow paths (see Appendix for a full derivation, and Table ref for a list of parameters used). The first-order differential equation governing transport and reaction is given as:

$$\phi \frac{\partial C}{\partial t} = -\omega \phi \frac{\partial C}{\partial z} + R_n(1-f) \quad (6)$$

Where  $C$  is the elemental concentration,  $\omega$  is the fluid velocity,  $\phi$  is the rock porosity,  $z$  is a position along the flow path,  $R_n$  is the rate of reaction, and  $f$  is the fraction of Si present in the dissolved load that is reprecipitated in the back reaction. The equation can be nondimensionalised using the Damköhler number ( $N_D$ ), which describes the relative importance of kinetic vs transport-controlled settings (Bethke, 2008):

$$N_D = \frac{R_n h}{\phi C_0 \omega} \quad (7)$$

Assuming steady-state ( $\partial C / \partial t = 0$ ), the concentration at the end of the flow path can be rearranged to give the residence time  $T_f$ :

$$T_f = \frac{(C - C_0)\phi}{(1 - f)R_n} \quad (8)$$

<b>Fontorbe</b>			
<b>Parameter</b>	<b>Definition</b>	<b>Units</b>	<b>Formula (Value)</b>
$\phi$	Porosity	-	0.1*
$\omega$	Fluid velocity	m/s	Variable
$h$	Length of flow path	m	Variable
$C$	Concentration end of flow path	$\mu\text{mol/L}$	Variable
$C_0$	Initial concentration	$\mu\text{mol/L}$	Rain Input
$f$	Fraction reprecipitated	-	0.5*
$N_D$	Damkohler Number	-	$N_D = \frac{R_n h}{\phi C_0 \omega}$
$T_f$	Residence time	s	$T_f = \frac{h}{\omega \phi}$
$R_n$	Reaction rate	$\text{mol}/\text{m}^3/\text{s}$	$\rho \cdot 10^6 \cdot k \cdot S \cdot X$
$k$	Reaction rate constant	$\text{mol}/\text{m}^2/\text{s}$	$10^{-15*}$
$S$	Specific surface area	$\text{m}^2/\text{g}$	0.1*
$\rho$	Plagioclase density	$\text{g}/\text{cm}^3$	2.7*
$X$	Volume fraction of mineral in rock	$g_{min}/g_{rock}$	0.2*

Table 2: Key parameters and definitions for the Fontorbe model. Starred terms are values used for calculation.

## Maher and Chamberlain (2014) Model

This model is built in accordance with the principle that the main control on silicate weathering is the residence time of the water. The model is based on the assumption that the reaction rate decreases linearly with approach to equilibrium, and that all weathering paths approach equilibrium. The motivation behind the hydrological control is based on sensitivity analyses of real catchment data on one-dimensional reactive transport models which suggest that porosity, mineral surface area, and temperature have no consistent correlation with water composition (Maher, 2011). See Appendix and Table ref for a full derivation and the model parameters respectively. The model begins with the following representation of the concentration of a solute in a fluid flow path:

$$\frac{dC}{dt} = -\frac{q}{\theta} \frac{dC}{dz} + \sum_i \mu_i R_{d,i} \left(1 - \left(\frac{C}{C_{eq}}\right)^{n_i}\right)^{m_i} - \sum_i \mu_i R_{p,i} \left(1 - \left(\frac{C}{C_{eq}}\right)^{n_i}\right)^{m_i} \quad (9)$$

Where  $C$  is the concentration,  $q$  is the fluid flux,  $\theta$  is the volumetric water content,  $z$  is the position along the flow path,  $\mu$  is the stoichiometric coefficient,  $R$  is the rate of reaction for dissolution and precipitation respectively,  $C_{eq}$  is the equilibrium concentration, and  $n$  and  $m$  are non-linear parameters (Maher and Chamberlain, 2013). For a given packet of water,  $R_n$  is defined as:

$$R_n = R_d - R_p \quad (10)$$

$$\frac{dc}{dt} = R_n \left(1 - \frac{C}{C_{eq}}\right) \quad (11)$$

Where  $R_d$  and  $R_p$  are the rates of dissolution and precipitation respectively. This can be solved for concentration, and rearranged for residence time to obtain:

$$T_f = \frac{C_{eq} \cdot (C - C_0)}{e^2 R_n (C_{eq} - C)} \quad (12)$$

Note the  $e^2$  term is used because the Maher model considers all paths as if they approach equilibrium.

<b>Maher</b>			
<b>Parameter</b>	<b>Definition</b>	<b>Units</b>	<b>Formula (Value)</b>
$\phi$	Porosity	-	0.1*
$h$	Length of flow path	m	Variable
$q$	Flow rate	m/s	Variable
$C_{eq}$	Equilibrium concentration	$\mu\text{mol/L}$	Max Catchment
$C_0$	Initial concentration	$\mu\text{mol/L}$	Rain Input
$R_n$	Net reaction rate	$\text{mol/L/s}$	$\rho \cdot 10^6 \cdot k \cdot S \cdot X$
$\rho$	Plagioclase density	$\text{g/cm}^3$	2.7*
$k$	Reaction rate constant	$\text{mol/m}^2/\text{s}$	$10^{-15*}$
$S$	Specific surface area	$\text{m}^2/\text{g}$	0.1*
$X$	Volume fraction of mineral in rock	$g_{min}/g_{rock}$	0.2*
$\tau$	Scaling factor	-	$\tau = e^2$
$D_w$	Damkohler Coefficient	$\text{m}^2/\text{s}$	$D_w = \frac{L\phi R_n}{C_{eq}}$
$T_f$	Residence time	s	$T_f = \frac{h\phi}{q}$

Table 3: Key parameters and definitions for the Maher model. Starred terms are values used for calculation.

## 4.4 Estimates of Uncertainty

Uncertainties were propagated using a Monte Carlo method using an assumed normal distribution. Both the observed parameters and estimated parameters have uncertainties associated to them.

Parameter Definitions and Propagated Uncertainties				
Parameter	Definition	Units	Value	Uncertainty
$\phi$	Porosity	-	0.1	$\pm 10\%$
$C_{eq}$	Equilibrium DSi concentration	$\mu\text{mol/L}$	$869 \mu\text{mol/L}$	$\pm 10\%$
$C_0$	Initial DSi concentration	$\mu\text{mol/L}$	$95 \mu\text{mol/L}$	$\pm 10\%$
$\rho$	Plagioclase density	$\text{g/cm}^3$	2.7	$\pm 10\%$
$k$	Reaction rate constant	$\text{mol/m}^2/\text{s}$	$10^{-15}$	$\pm 10\%$
$S$	Specific surface area	$\text{m}^2/\text{g}$	0.1	$\pm 10\%$
$X$	Volume fraction of mineral in rock	$\text{g}_{\text{min}}/\text{g}_{\text{rock}}$	0.2	$\pm 10\%$
$f$	Fraction reprecipitated	-	0.5	$\pm 10\%$
$\Delta G^0$	Standard Gibbs Free Energy	$\text{kJ/mol}$	$-\text{RTlnK}^*$	$\pm 10\%$

Table 4: Key parameters, definitions, and propagated uncertainties. \* Uncertainty associated with temperature and K calculated from pgcc using The Geochemist's Workbench® Rxn program(ref)

# 5 Results: Differences in Spring Chemistry and Residence Time

## 5.1 Traverse 1

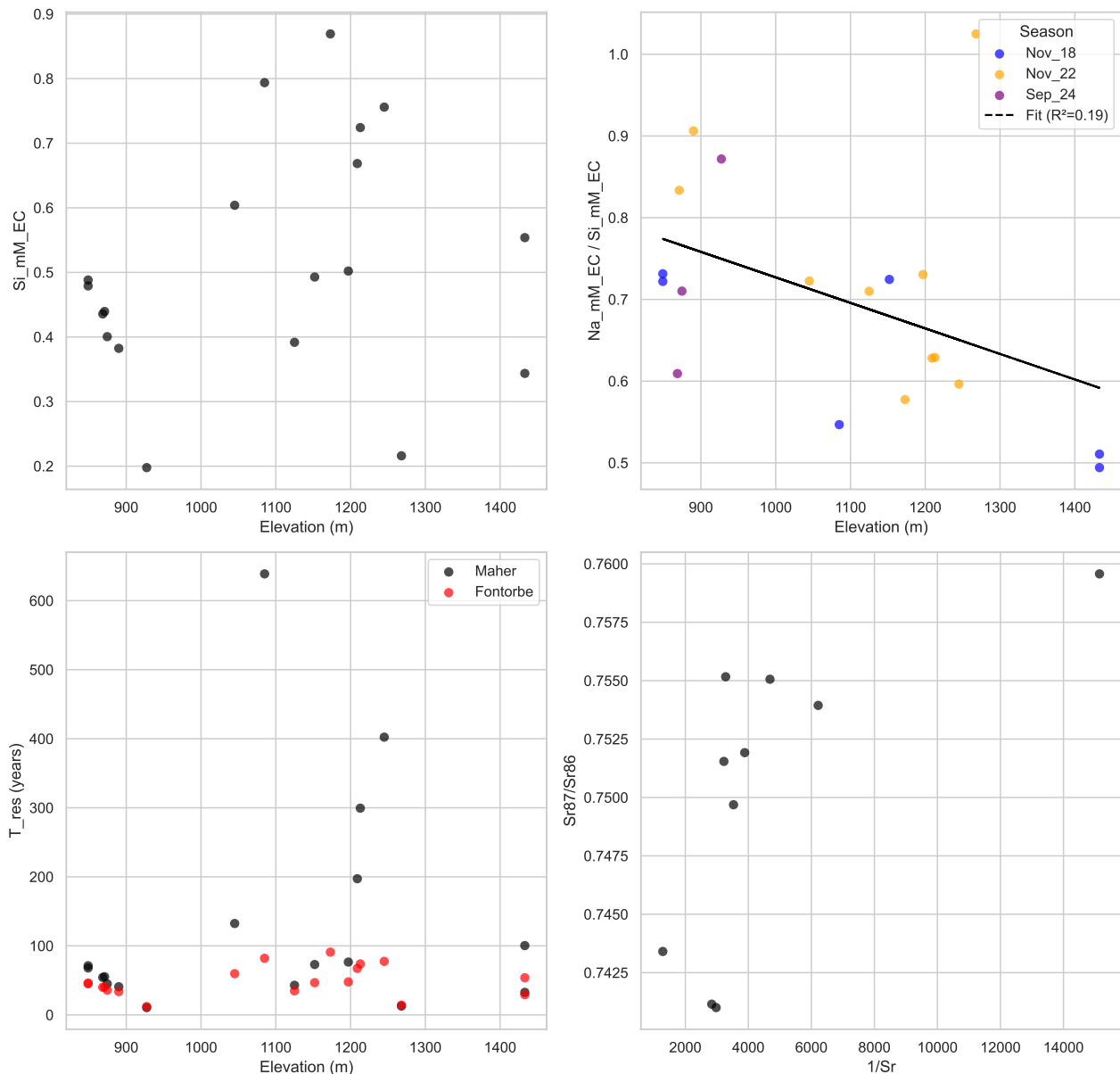


Figure 3: Traverse 1 - Variations in Spatial Chemistry

Concentration of dissolved silicon (DSi) in the springs sampled in Traverse 1 is at a maximum for the whole catchment. There is no clear trend of increasing DSi concentration with decreasing elevation, but Na/Si does increase with the same x-axis. The Fontorbe model

predicts a peak of  $\approx 100$  years, while the Maher model predicts a much higher residence time of  $\approx 600$  years.

## 5.2 Traverse 2

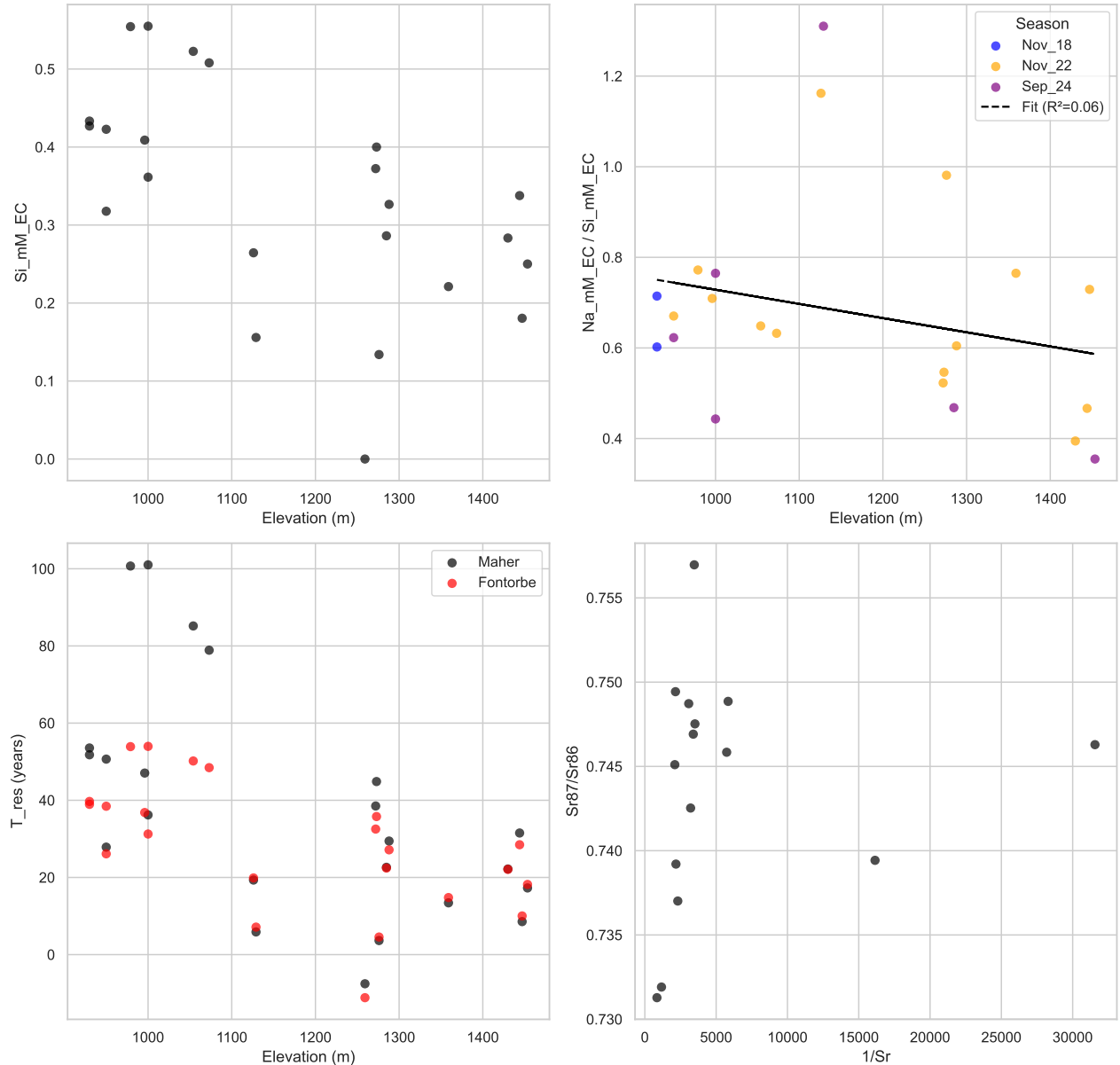


Figure 4: Traverse 2 - Variations in Spatial Chemistry

Dissolved silicon concentration shows a clear increase in concentration with decreasing elevation. There is no resolvable trend with  $\text{Na}/\text{Si}$  and elevation, nor with different seasons when it was collected. Residence times are generally lower than those in Traverse 1, but the Maher model is still higher at lower elevations, predicting a maximum of  $\approx 100$  years. The Fontorbe model predicts generally older times than the Maher model at higher elevations, and lower times at lower elevations.

### 5.3 Traverse 3

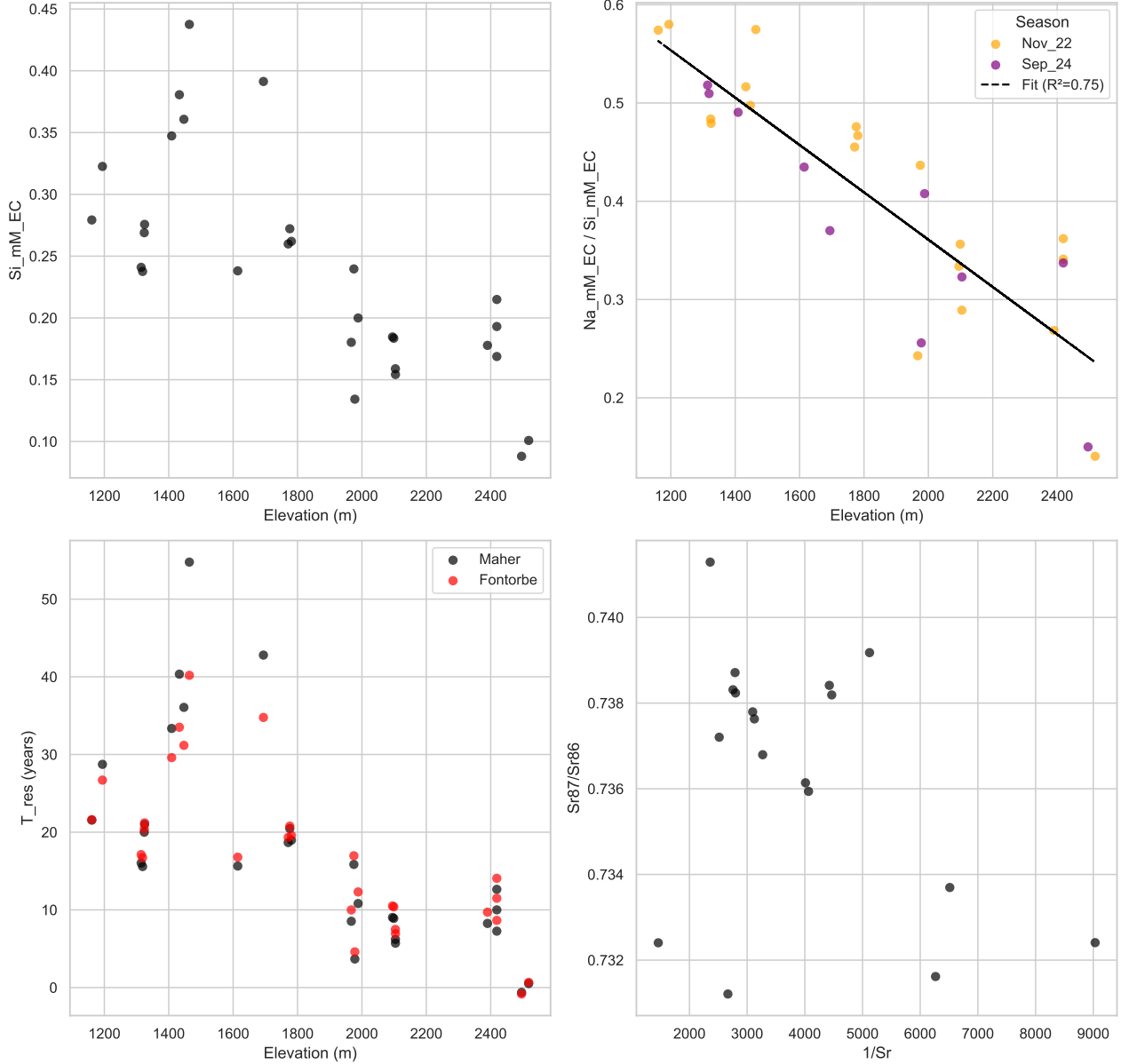


Figure 5: Traverse 3 - Variations in Spatial Chemistry

Dissolved silicon concentration increases with decreasing elevation in Traverse 3. There is a potential dip at the lowermost elevation sampled. Na/Si showcases a consistent increase with decreasing elevation, and this trend carries through between different seasons. Residence times predicted increase as elevation decreases, peaking at  $\approx 50$  years for the Maher model. At the very end of the flow path, however, both the Maher and Fontorbe model predict  $\approx 25$  years.

## 5.4 Traverse 4

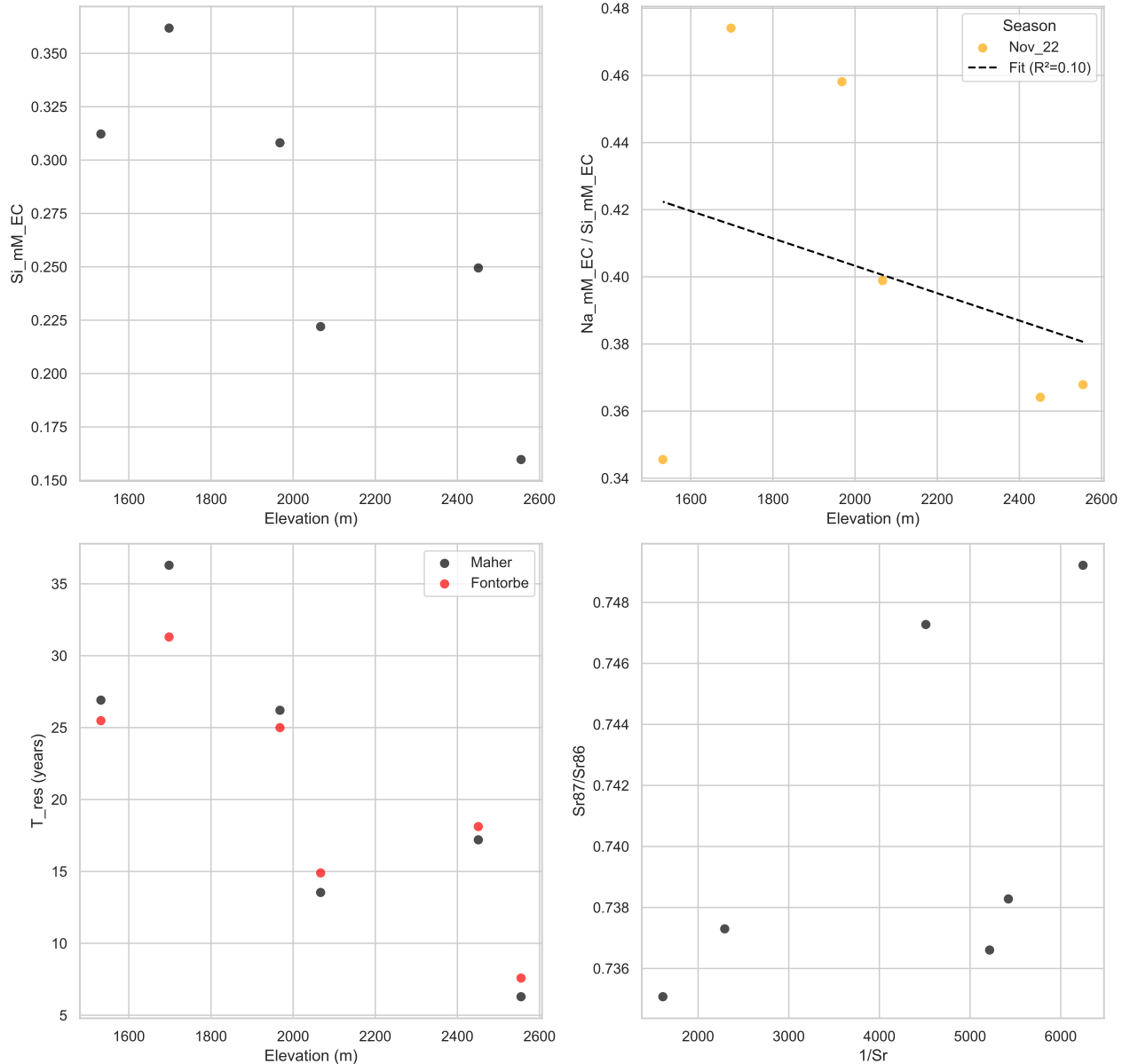


Figure 6: Traverse 4 - Variations in Spatial Chemistry

Traverse 4 is undersampled compared to the other traverses. Given the small sample set, any apparent trend is less likely to be reflective of the true chemistry. Nevertheless, DSi increases with decreasing elevation as seen in some of the previous traverses. There is no discernable trend with Na/Si. Residence times also increase with decreasing elevation, with the Maher model predicting younger times at the highest elevations, and older times at the lowest elevations. The highest residence times predicted are  $\approx 35$  years.

## 5.5 Traverse 5

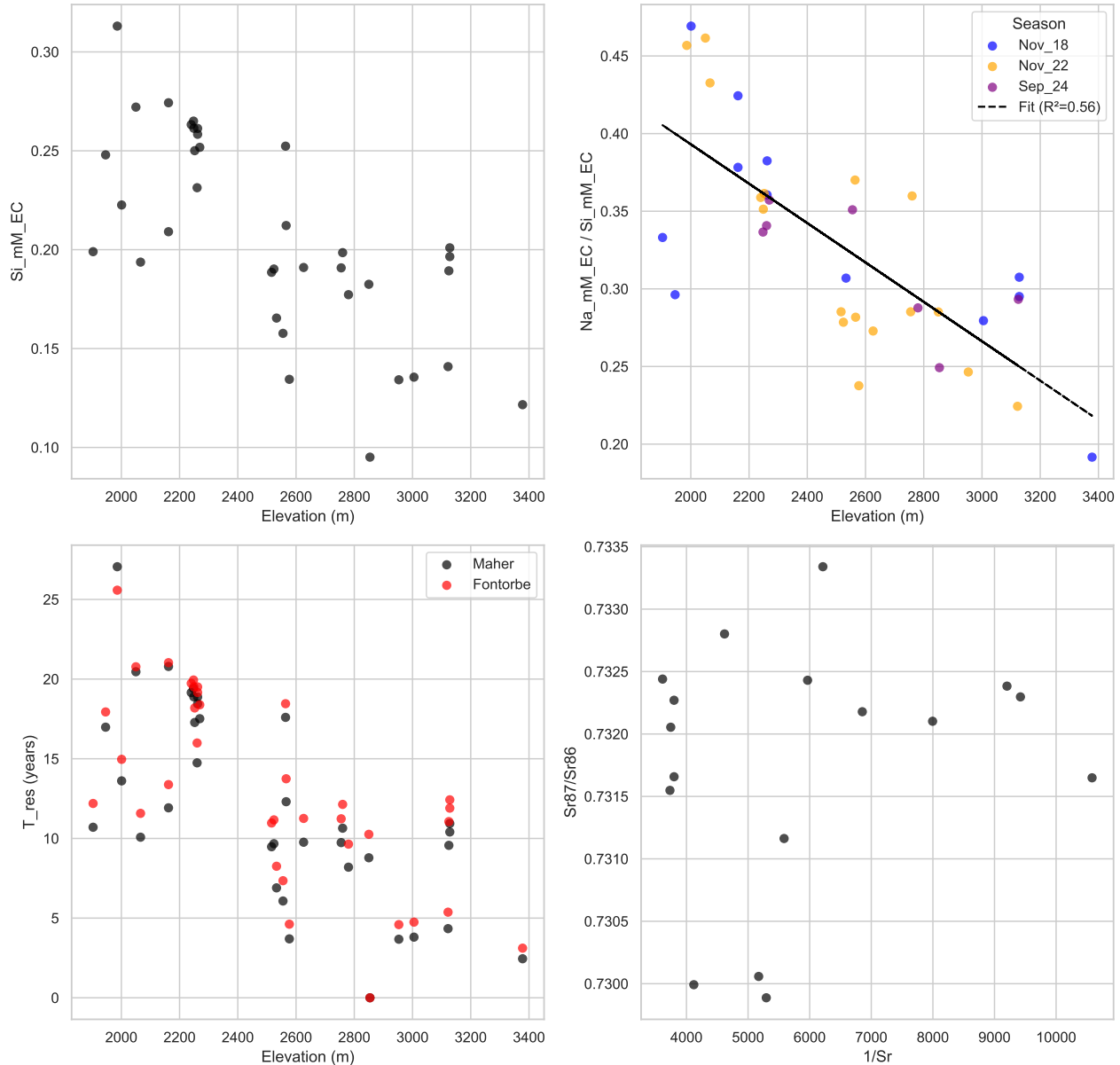


Figure 7: Traverse 5 - Variations in Spatial Chemistry

Traverse 5 is highly sampled and sits at the highest elevation of the whole catchment. DSi concentration increases with decreasing elevation but there is noticeable scatter in the data. Na/Si similarly shows a trend of increasing ratio with decreasing elevation, and it is replicated between different seasons, with considerable scatter. Residence times are the lowest predicted in the catchments.

## 5.6 Time Series Trends

Concentrations of dissolved silicon in several springs in the catchment show a consistent decrease in concentration with the onset of the monsoon. Concentrations are high in April, decrease to a minimum in September, then slowly increase back to April levels through October and November. Decrease in concentration is likely a sign of dilution from increased precipitation during the monsoon. Such a trend is also present in a time series of a spring in Traverse 3. The average April-September decrease is small compared to the average dissolved silicon concentration of the rain.

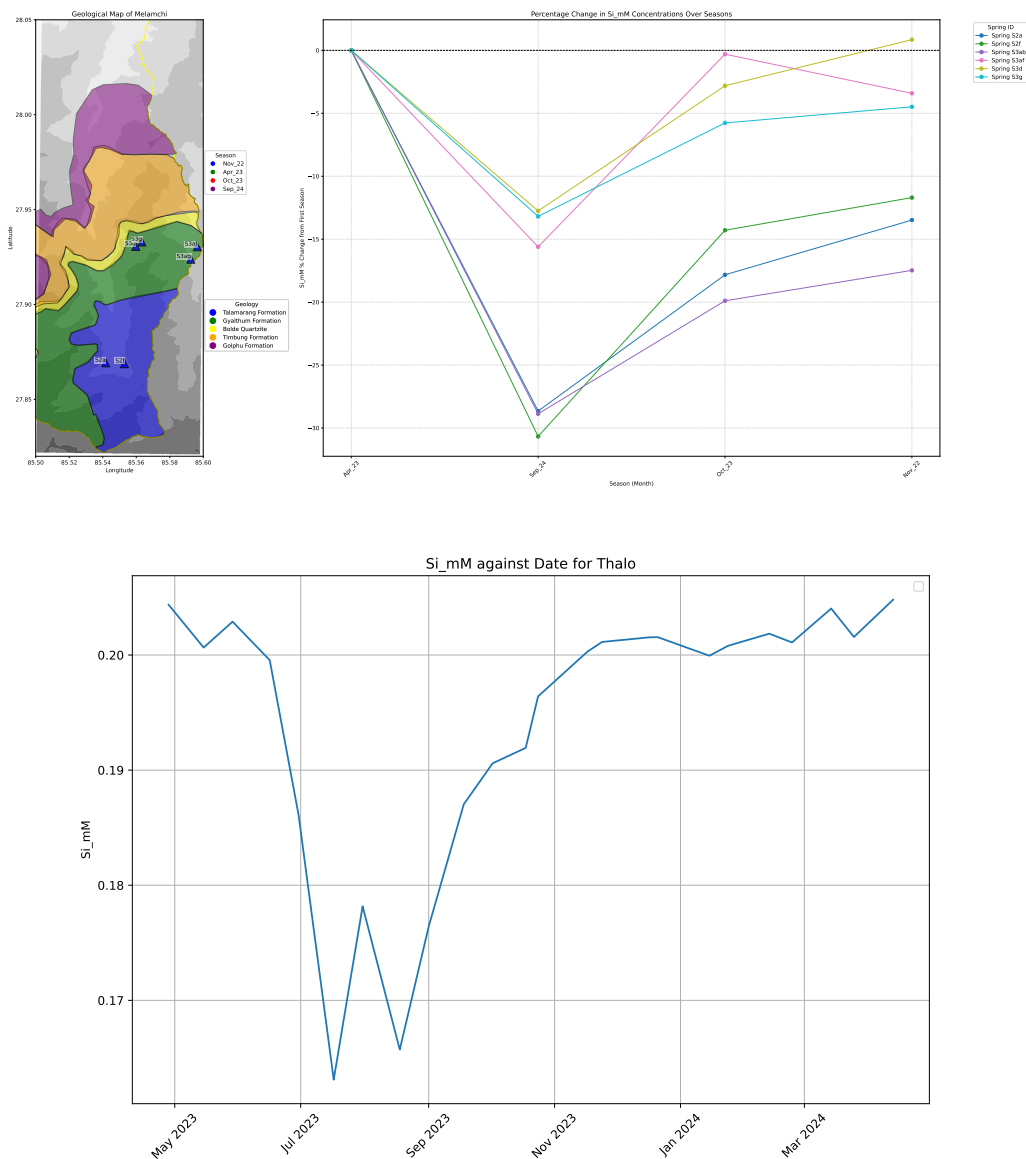


Figure 8: Seasonal changes in spring concentration indicating monsoonal precipitation influence.; Time series of spring concentration changes over time.

## **5.7 Strontium Isotope Values of Springs and Rain**